JACS
JOURNAL OF THE AMERICAN CHEMICAL SOCIETY

COMMUNICATION

pubs.acs.org/JACS

Thermodynamics, Kinetics, and Photochemistry of β-Strand Association and Dissociation in a Split-GFP System

Keunbong Do and Steven G. Boxer*

Department of Chemistry, Stanford University, Stanford, California 94305-5080, United States

Supporting Information

ABSTRACT: Truncated green fluorescent protein (GFP) that is refolded after removing the 10th β-strand can readily bind to a synthetic strand to recover the absorbance and fluorescence of the whole protein. This allows rigorous experimental determination of thermodynamic and kinetic parameters of the split system including the equilibrium constant and the association/dissociation rates, which enables residue-specific analysis of peptide−protein interactions. The dissociation rate of the noncovalently bound strand is observed by strand exchange that is accompanied by a color change, and surprisingly, the rate is greatly enhanced by light irradiation. This peptide−protein photodissociation is a very unusual phenomenon and can potentially be useful for introducing spatially and temporally well-defined perturbations to biological systems as a genetically encoded caged protein.

Split green fluorescent proteins (GFPs), along with other split reporter proteins, have been developed as probes to study protein−protein interactions and protein localization in cells.[1−3] The spontaneous reassembly of split proteins[4,5] can also be used to generate semisynthetic proteins *in vitro*, in which the smaller fragment can be prepared with complete synthetic control.[6] We introduced the method and notation illustrated in Figure 1, which can be generally applied to any secondary structural element of GFP, that is, to all 11 β-strands and the central helix containing the chromophore.[7] A circularly permuted GFP is expressed with a protease cleavage site inserted in a loop added between the secondary structural element to be removed and the rest of the protein (see Supporting Information, SI, for design criteria). Then, the cleavage site is cut, and the secondary structural element is removed by size exclusion chromatography in denaturing conditions to obtain the truncated protein. Interestingly, when the truncated GFP with the 11th strand removed, GFP:~~loop:s11~~, is refolded, the chromophore undergoes thermal *cis*-to-*trans* isomerization.[8] Strand 11 does not bind to the *trans* truncated GFP, but binds only to the *cis* truncated GFP after making a photostationary mixture of *cis* and *trans* truncated GFPs. While this light-driven reassembly is potentially useful in cell biology, it complicates kinetic and thermodynamic studies of the reassembly process. By contrast, we show in the following that the truncated GFP refolded with the 10th strand removed (~~s10:loop~~:GFP[9] in Figure 1) binds to strand 10 without such complications, permitting direct and quantitative measurement of the reassembly process. Furthermore, strand 10 contains threonine 203 that causes a red shift upon mutation to tyrosine (T203Y), which is the basis of the widely used class of yellow fluorescent proteins (YFPs),[10] and which provides a convenient way of probing strand replacement as illustrated by the color code in Figure 1.

Figure 2A compares the absorbance and the fluorescence emission spectra before and after the complex formation between $\underline{s10}^{203T}$ and ~~s10:loop~~:GFP, where both the absorbance and the fluorescence spectra become nearly indistinguishable from those of the uncut protein (s10:loop:GFP) once the complex is formed (see SI for comparison). Upon complex formation, both protonated and deprotonated absorbance bands respectively at 389 and 465 nm[11] are slightly red-shifted to 393 and 467 nm with an isosbestic point around 410 nm. The truncated protein is only weakly fluorescent, and the fluorescence quantum yield shows a very large increase (about 25-fold for 390 nm excitation and 505 nm emission) when the peptide binds. The spectral shift and dramatic increase in fluorescence quantum efficiency are very useful for the acquisition of kinetic and thermodynamic data of the reassembly process and may be further exploited in imaging applications. Very weak fluorescence is reminiscent of what is observed for the isolated chromophore[13] suggesting that removal of strand 10 results in conformational flexibility that leads to nonradiative decay. By comparison, when strand 11 is removed, the absorbance spectrum changes substantially as the *trans* form of the chromophore is formed and fluorescence is only reduced by a factor of 3.[8] Figure 2B and 2C show the absorbance change of ~~s10:loop~~:GFP when it is titrated with $\underline{s10}^{203T}$ or $\underline{s10}^{203Y}$ to reform GFP or YFP, respectively.

The equilibrium constant of the binding reaction was measured using fluorescence quantum yield recovery as an indication for the complex formation. Figure 3 is a plot of the fluorescence intensity as a function of the total concentration of $\underline{s10}^{203Y}$ mixed with 2 nM ~~s10:loop~~:GFP. The data were fit to the analytical solution of a one-to-one binding reaction, giving a dissociation constant (K_d) of 78.7 ± 13.8 pM. In a similar manner, K_d = 139.1 ± 20.1 pM was determined for $\underline{s10}^{203T}$ (data not shown). These K_d values are much smaller than the value reported for strand 7 complementation (531 nM)[14] and even smaller than the lowest value reported for the fragment complementation in the 10th type III domain of human fibronectin (1.5 nM in the presence of 750 mM glycerol), which is one of the highest affinities reported for protein−protein interactions involving β-strands.[15]

The K_d values were too small to be precisely measured by isothermal calorimetry given the small heat generated per binding reaction, but the standard enthalpy of reaction (ΔH°) could be

Received: August 23, 2011
Published: October 07, 2011

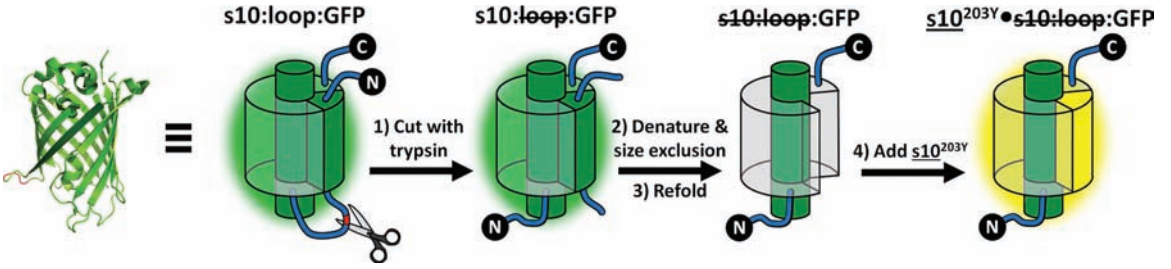

Figure 1. Schematic of strand removal and reassembly based on circularly permuted GFP focusing on the 10th β-strand. Following the systematic notation previously developed,[7] circularly permuted GFP with strand 10 at its N-terminus connected to the rest of the protein through a loop sequence containing a protease cleavage site is denoted as s10:loop:GFP (the ordering of elements is always from N- to C-terminus). A strike through loop (s10:~~loop~~:GFP) indicates the protease cleavage site was cut, an additional strike through s10 (~~s10:loop~~:GFP) indicates that the native strand 10 was removed and that the truncated protein is refolded, and an underlined s10 (s10) refers to an added synthetic strand 10 that forms a complex with the truncated GFP, in this case containing the T203Y mutation that changes the color of the reassembled protein as in YFP. Note that although ~~s10:loop~~:GFP in the diagram is shown as a cylinder with a strand simply removed, the actual structure is not known; similarly, although the β-strands are presented as wedges, their secondary structure is likely to change after binding to the truncated GFP. The GFP cartoon on the left is adapted from the PDB structure of superfolder GFP (2B3P).

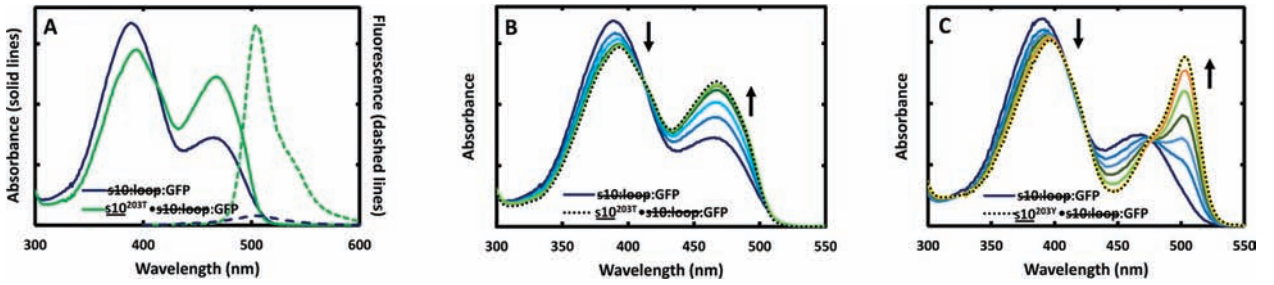

Figure 2. Reconstitution of GFP from s10 and ~~s10:loop~~:GFP. (A) Absorbance and fluorescence spectra of ~~s10:loop~~:GFP (dark blue) and s10^{203T}•~~s10:loop~~:GFP (green). All spectra are normalized by concentration so that relative absorbance and fluorescence intensity directly translate to the relative extinction coefficient and the product of extinction coefficient and fluorescence quantum yield. (B) Absorbance change of ~~s10:loop~~:GFP (dark blue) upon addition of s10^{203T} aliquots. (C) Absorbance change of ~~s10:loop~~:GFP upon addition of s10^{203Y} aliquots. In (B) and (C), arrows indicate the direction of spectral changes as more peptide is added, and the dotted curves are the spectra of purified GFP or YFP complex, normalized at the isosbestic points, showing the expected final spectra upon reconstitution.

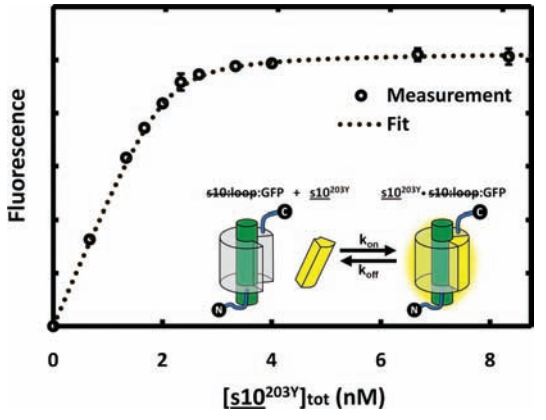

Figure 3. Fluorescence binding titration of 2nM ~~s10:loop~~:GFP with s10^{203Y}. The sample was excited at 500 nm, and emission was collected at 520 nm. Each data point is an average of four different sample measurements, and error bars indicate standard deviation.

obtained by measuring the total heat released from a single injection of s10 (4.3 molar excess) into 1.4 mL of 500 nM ~~s10:loop~~:GFP. The resulting ΔH° was then used with the equilibrium constant to obtain ΔS°; all values are summarized in Table 1. It is notable that there is an apparent enthalpy−entropy compensation for T203Y substitution that leads to a relatively small difference in the free energy of binding ($\Delta\Delta G^\circ = \Delta G^\circ_{203Y} - \Delta G^\circ_{203T} = -0.34 \pm 0.13$ kcal·mol^{-1}) despite the large difference in ΔH° ($\Delta\Delta H^\circ = \Delta H^\circ_{203Y} - \Delta H^\circ_{203T} = -10.38 \pm 2.36$ kcal·mol^{-1}). Since the only difference between the two systems is the T203Y substitution, this provides an estimate of the energetic consequences of a single side-chain difference; further work using natural and unnatural amino acids will be reported separately.

As shown in Figure 4, the association (on-) rate of s10 and ~~s10:loop~~:GFP was measured using fluorescence recovery with great care not to expose the sample to any more light than needed for the reasons discussed below.[16] Kinetic fits were performed with Berkeley Madonna[17] by numerically solving the differential equations of a bimolecular reaction. From the fits, bimolecular rate constants of 4232 ± 163 and 5658 ± 135 M^{-1} s^{-1} were determined respectively for s10^{203T} and s10^{203Y} binding (Table 1). These association rates are about 30-fold faster than that reported for strand 11 association to the *cis* form of GFP: ~~loop:s11~~.[8]

When the GFP complex, s10^{203T}•~~s10:loop~~:GFP, was mixed with excess s10^{203Y}, the absorbance shifted very slowly from that of GFP to that of YFP as shown in Figure 5B (the spectral shift occured in the other direction, from the YFP to the GFP

Table 1. Thermodynamic and Kinetic Parameters of s10•~~s10:loop~~:GFP Interaction at 25 °C, 1 atm

s10 peptide	K_d[a] (pM)	$\Delta G°$[b] (kcal·mol^{-1})	$\Delta H°$ (kcal·mol^{-1})	$\Delta S°$ (cal·mol^{-1}·K^{-1})	k_{on} ($M^{-1}·s^{-1}$)	k_{off} (s^{-1})	K_d[c] (pM)
s10^{203T}	139.1	−13.43	−26.29	−43.16	4232	6.08×10^{-7}	143.8
	±20.1	±0.09	±1.46	±4.90	±163	$\pm 6.6 \times 10^{-8}$	±16.5
s10^{203Y}	78.7	−13.77	−36.67	−76.86	5658	3.43×10^{-7}	60.65
	±13.8	±0.10	±1.86	±6.25	±135	$\pm 2.07 \times 10^{-7}$	±36.64

[a] From direct titration. [b] Calculated from K_d[a]. [c] From k_{off}/k_{on} ratio.

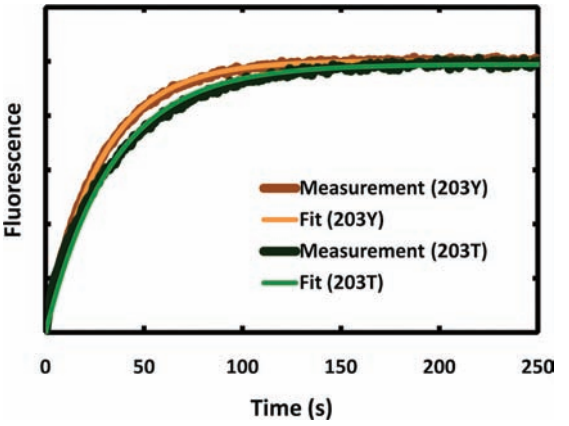

Figure 4. Binding kinetics of 50nM ~~s10:loop~~:GFP and 7 μM s10. Emission at 505 nm for s10^{203T} reassembly and 520 nm for s10^{203Y} reassembly was monitored while exciting at 390 nm.

spectrum, when the YFP complex, s10^{203Y}•~~s10:loop~~:GFP, was mixed with excess s10^{203T}; data not shown). This indicates that a noncovalently bound strand can be spontaneously replaced by an added strand without denaturing the protein. The exchange process can be described with a simple two-step model as schematically illustrated in Figure 5A: first, the native strand dissociates, and second, the different strand binds to the truncated protein.[18]

Taking advantage of the spectral shift accompanying the peptide exchange, the dissociation (off-) rates of the complexes could be estimated by adding the different peptide in excess. For example, 1.3 μM s10^{203T}•~~s10:loop~~:GFP and 30 μM s10^{203Y} were mixed, and gradual conversion of GFP to YFP was observed with a half-life of about 300 h (Figure 5B, see SI). Since the half-life of the YFP complex formation process (~~s10:loop~~:GFP + s10^{203Y} → s10^{203Y}•~~s10:loop~~:GFP) would be only 4 s in 30 μM s10^{203Y}, the dissociation step of the exchange process must be rate-limiting, and thus the dissociation rate can be estimated directly from the exchange rate (Table 1). Using the ratio of the dissociation and the association rates, K_d values of 143.8 ± 16.5 pM for s10^{203T} and 60.65 ± 36.64 pM for s10^{203Y} were obtained, which agree with the K_d values obtained from the binding isotherm within their error. Thus, the peptide exchange process appears to be well described by the scheme suggested in Figure 5A.

Surprisingly, the peptide exchange rate was dramatically enhanced by light irradiation. As shown by comparing Figure 5B and 5C, the apparent exchange rate was up to 3000 times faster in the presence of light, suggesting that the rate-limiting step of the exchange process, the dissociation of s10^{203T} in this case, is effectively accelerated by light. Figure 5D is a plot of the peptide exchange rate as a function of the power of a 405 nm cw diode laser

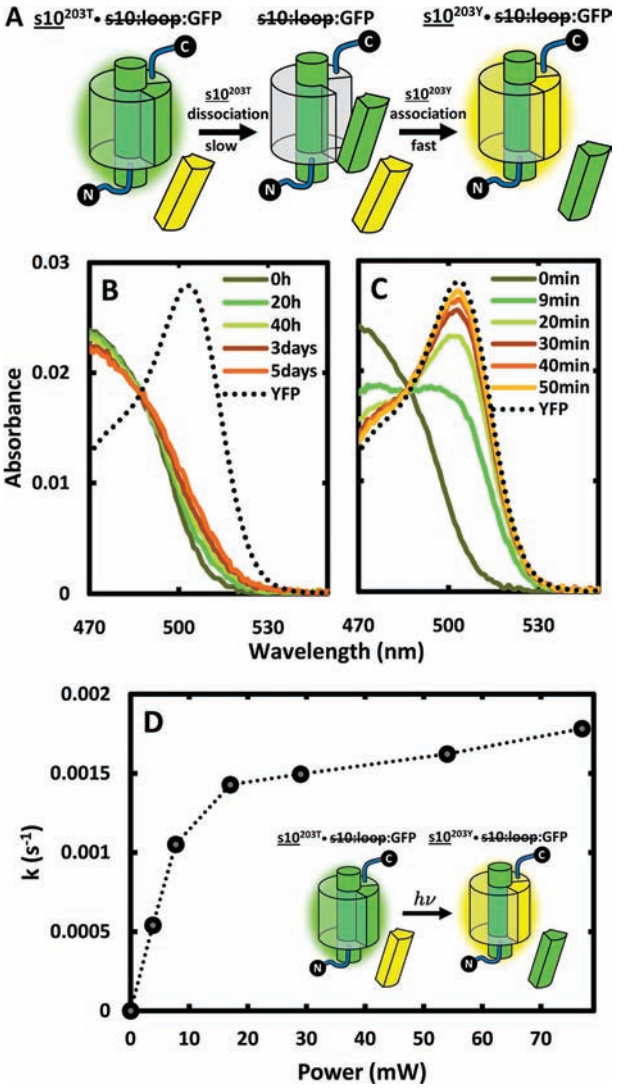

Figure 5. (A) Schematic illustration of the peptide exchange process leading to color change (the yellow wedge represents the excess s10^{203Y}). (B) Absorbance change of 1.3 μM s10^{203T}•~~s10:loop~~:GFP and 30 μM s10^{203Y} mixture in the dark observed over 5 days ($t_{1/2} \approx 300$ h) and (C) with 17 mW of 405 nm light irradiation for 50 min ($t_{1/2}$ = 8 min). (D) Pseudo-first-order peptide exchange rate versus the 405 nm laser power.

irradiating a 3 mL mixture of 1.3 μM s10^{203T}•~~s10:loop~~:GFP and 30 μM s10^{203Y} that is constantly stirred. It can be seen that the rate increases linearly in the lower power range and levels off at higher power. The quantum yield of the peptide exchange process was approximately 0.2 % in the linear region (up to about 10 mW) of the plot (see SI for the calculation).

dx.doi.org/10.1021/ja207985w |J. Am. Chem. Soc. 2011, 133, 18078–18081

When either of the complexes, s10^{203T}•~~s10:loop~~:GFP or s10^{203Y}•~~s10:loop~~:GFP, was exposed to 405 nm light *without* adding extra peptide in solution, the absorbance spectrum shifted toward that of ~~s10:loop~~:GFP and the fluorescence intensity decreased accordingly (cf. Figure 2A). Assuming that the peptide photodissociates from the truncated protein to give a mixture of the complex and the dissociated species, the equilibrium composition in the presence of light could be properly predicted with the measured association rates (Table 1) and the light-enhanced dissociation rates (see SI). Once the irradiation was stopped, absorbance and fluorescence returned to those of the starting complex over time. Furthermore, when a bimolecular reaction model was numerically fit to the absorbance and fluorescence recovery data, rate constants of 4205 ± 576 and $5606 \pm 303\ M^{-1}\ s^{-1}$ were determined respectively for the GFP and the YFP complex, which is within the error of the independently measured association rate of each peptide (Table 1). This agreement suggests that the light irradiation is indeed facilitating the peptide to dissociate.

The elementary mechanism of this unique peptide−protein photodissociation process is unknown at this time, but we can speculate on what might be happening based on the previous study of GFP:~~loop:s11~~.[8] Similar to GFP:~~loop:s11~~ which binds to strand 11 only with the *cis* configuration of the chromophore, it is possible that the chromophore in s10•~~s10:loop~~:GFP is in the *cis* configuration and undergoes rapidly reversible *cis*-to-*trans* isomerization upon photoexcitation, where the putative *trans* s10•~~s10:loop~~:GFP has an enhanced dissociation rate for strand 10. Further study to explore this mechanism is underway, and it may be possible to enhance the efficiency of the light-driven process through judicious modification of the protein such as incorporating well-known mutations that facilitate *cis*−*trans* isomerization[19−22] or by random screening. Such light-driven dissociation of a GFP peptide can potentially be an effective way of introducing perturbations to a biological system with high spatial and temporal resolution. Furthermore, spectral shifts caused by mutations such as T203Y would allow reversible and orthogonal enhancement of s10^{203T} and s10^{203Y} dissociation. Finally, it is evident from these results and the earlier work on strand 11[8] that all measurements of the intrinsic properties in split-GFP systems must be conducted with careful control of light levels.

To conclude, we have shown that the split-GFP scheme, with its built-in fluorescent reporter, provides a reliable and convenient platform to experimentally extract kinetic and thermodynamic information of a split system, with access to complete synthetic flexibility on a given strand. Further application of the scheme to synthetic strands with systematic variations can provide insights into peptide−protein interactions involving β-strands in general[23] as well as the design of split-GFPs with desired properties. In addition, the light-driven peptide dissociation revealed from the dissociation rate measurement opens new possibilities of developing the system into a genetically encoded caged protein that may enable manipulation and detection of protein interactions in cells.

■ ASSOCIATED CONTENT

Supporting Information. Protein preparation, amino acid sequences, instrumentation, and basic methods. This material is available free of charge via the Internet at http://pubs.acs.org.

■ AUTHOR INFORMATION

Corresponding Author
sboxer@stanford.edu

■ ACKNOWLEDGMENT

We thank Kevin Kent and Luke Oltrogge for many helpful discussions and comments. This research was supported in part by a grant from the NIH (GM27738), and K.D. is supported by a John Stauffer Stanford Graduate Fellowship and the Korea Foundation for Advanced Studies.

■ REFERENCES

(1) Ghosh, I.; Hamilton, A. D.; Regan, L. *J. Am. Chem. Soc* **2000**, *122*, 5658–5659.
(2) Magliery, T. J.; Wilson, C. G. M.; Pan, W.; Mishler, D.; Ghosh, I.; Hamilton, A. D.; Regan, L. *J. Am. Chem. Soc.* **2005**, *127*, 146–157.
(3) Michnick, S. W.; Ear, P. O.; Manderson, E. N.; Remy, I.; Stefan, E. *Nat. Rev. Drug. Discov.* **2007**, *6*, 569–582.
(4) Richards, F. M. *Proc. Natl. Acad. Sci. U.S.A.* **1958**, *44*, 162–166.
(5) Carey, J.; Lindman, S.; Bauer, M.; Linse, S. *Protein Sci.* **2007**, *16*, 2317–2333.
(6) Kent, K. P.; Childs, W.; Boxer, S. G. *J. Am. Chem. Soc.* **2008**, *130*, 9664–9665.
(7) Kent, K. P.; Oltrogge, L. M.; Boxer, S. G. *J. Am. Chem. Soc.* **2009**, *131*, 15988–15989.
(8) Kent, K. P.; Boxer, S. G. *J. Am. Chem. Soc.* **2011**, *133*, 4046–4052.
(9) This notation will refer only to the refolded form in this communication.
(10) Tsien, R. Y. *Annu. Rev. Biochem.* **1998**, *67*, 509–44.
(11) Chattoraj, M.; King, B. A.; Bublitz, G. U.; Boxer, S. G. *Proc. Natl. Acad. Sci. U.S.A.* **1996**, *93*, 8362–83667.
(12) Pedelacq, J.; Cabantous, S.; Tran, T.; Terwilliger, T. C.; Waldo, G. S. *Nat. Biotechnol.* **2006**, *24*, 79–88.
(13) Niwa, H.; Inouye, S.; Hirano, T.; Matsuno, T.; Kojima, S.; Kubota, M.; Ohashi, M; Tsuji, F. I. *Proc. Natl. Acad. Sci. U.S.A.* **1996**, *93*, 13617–13622.
(14) Huang, Y.; Bystroff, C. *Biochemistry* **2009**, *48*, 929–40.
(15) Dutta, S.; Batori, V.; Koide, A.; Koide, S. *Protein Sci.* **2005**, *14*, 2838–2848.
(16) Control measurements were performed to check that the result does not depend on light intensity or wavelength.
(17) Version 8.3.18, http://www.berkeleymadonna.com/.
(18) Strand exchange was not observed in the analogous system involving strand 11 both in the dark and with irradiation.[6]
(19) Patterson, G. H.; Lippincott-Schwartz, J. *Science* **2002**, *297*, 1873–1877.
(20) Chudakov, D. M.; Verkhusha, V. V.; Staroverov, D. B.; Souslova, E. A.; Lukyanov, S.; Lukyanov, K. A. *Nat. Biotechnol.* **2004**, *22*, 1435–1439.
(21) Ando, R.; Mizuno, H.; Miyawaki, A. *Science* **2004**, *306*, 1370–1373.
(22) Bizzarri, R.; Serresi, M.; Cardarelli, F.; Abbruzzetti, S.; Campanini, B.; Viappiani, C.; Beltram, F. *J. Am. Chem. Soc.* **2010**, *132*, 85–95.
(23) London, N.; Movshovitz-Attias, D.; Schueler-Furman, O. *Structure (Cambridge, MA, U. S.)* **2010**, *18*, 188–199.